Astron. Astrophys. 353, 741–748 (2000)

ASTRONOMY AND ASTROPHYSICS

Nonlinear dissipative spherical Alfvén waves in solar coronal holes

V.M. Nakariakov[1], **L. Ofman**[2], **and T.D. Arber**[3]

[1] Physics Department, University of Warwick, Coventry CV4 7AL, UK
[2] Raytheon ITSS/NASA Goddard Space Flight Center, 682, Greenbelt, MD 20771, USA
[3] School of Mathematical and Computational Sciences, University of St Andrews, St Andrews, Fife KY16 9SS, Scotland

Received 13 August 1999 / Accepted 22 October 1999

Abstract. The weakly nonlinear dynamics of linearly polarized, spherical Alfvén waves in coronal holes is investigated. An evolutionary equation, combining the effects of spherical stratification, nonlinear steepening and dissipation due to shear viscosity is derived. The equation is a spherical analog of the scalar Cohen–Kulsrud–Burgers equation. Three main stages of the wave evolution are distinguished: geometrical amplification, wave breaking and enhanced dissipation. The wave dissipation is dramatically increased by the nonlinear transfer of energy to smaller scales. The scenario of the nonlinear dissipation is practically independent of viscosity. The dissipation rate is stronger for highest amplitudes, and depends weakly on the wave period and the temperature of the atmosphere. Waves with periods less than 300 s and initial amplitudes about 2–3% of the Alfvén speed at the base of the corona are subject to the nonlinear steepening and dissipation in less than 10 solar radii. For the Alfvén waves with amplitudes less than 25 km s^{-1} at the base of the corona, the maximum amplitude of up to 200 km s^{-1} is reached at several solar radii. The nonlinear distortion of the wave shape is accompanied by the generation of longitudinal motions and density perturbations.

Key words: Magnetohydrodynamics (MHD) – waves – methods: analytical – Sun: corona – Sun: oscillations

1. Introduction

A possible role of magnetohydrodynamic (MHD) waves in accelerating the high speed solar wind and the heating of plasma in the open magnetic structures of the solar corona has been discussed since the pioneering works of Parker (1965). The presence of MHD waves in the open structures of the solar corona is now beyond doubt. Recently, upwardly propagating compressive waves were detected in polar plumes (DeForest & Gurman 1998) with SOHO EIT and interpreted as slow magnetoacoustic waves (Ofman et al. 1999); non-thermal broadening of coronal emission lines found with SOHO UVCS is most probably associated with MHD waves (Ofman & Davila 1997b, Ofman et al. 1998). Also, Alfvén waves are observed *in situ* further out in the polar solar wind as magnetic field fluctuations by the ULYSSES spacecraft (e.g. Balogh et al. 1995).

In this study, we concentrate our attention on the evolution of Alfvén waves during their propagation through the Sun's atmosphere.

A theory of Alfvén waves in coronal holes has to incorporate the effects of the spherical geometry and transversal structuring, along with nonlinear and dissipative effects. Some of these effects are already well-understood. In homogeneous plasmas, elliptically polarized plane Alfvén waves of a finite amplitude are described by the vector Cohen–Kulsrud equation (Cohen & Kulsrud 1974). Solutions of this equation show nonlinear self-interaction of the waves through forced density perturbations and longitudinal motions. Note that while circularly polarized Alfvén waves in the homogeneous plasmas are an exact, although unstable, nonlinear solution of magnetohydrodynamics, Alfvén waves of linear and elliptic polarization are not. They drive second-order fluctuations in velocity and density (see, e.g., Hollweg 1971), which leads to the self-interaction. Including dissipative processes into the model, Kennel et al. (1990) have generalized the Cohen–Kulsrud equation to the so-called Cohen–Kulsrud–Burgers equation. In particular, the Cohen–Kulsrud–Burgers equation describes evolution of the Alfvèn waves into a rotational discontinuity. In the limiting case of a linearly polarized wave, the pair of equations of Cohen–Kulsrud–Burgers decouples and waves of different polarization are described by two independent scalar equations. These are called the scalar Cohen–Kulsrud–Burgers equations.

In inhomogeneous plasmas, Alfvén waves are not the exact solution of the MHD set of equations and always evolve. Structuring of the plasma in the direction transverse to the magnetic field leads to Alfvén wave phase mixing (Heyvaerts & Priest 1983), accompanied by nonlinear generation of magnetoacoustic waves (Nakariakov et al. 1997, 1998). Obliquely propagating fast magnetoacoustic waves are generated with secular efficiency, while the slow wave generation is similar to the homogeneous case. However, the efficiency of fast wave generation is determined by the Alfvén wave amplitude, longitudinal wave number and steepness of the transverse inhomogeneity. Consequently, if the transverse gradients are not very high, this effect can be neglected in an initial stage, with respect to the generation of slow waves.

Send offprint requests to: V.M. Nakariakov (valery@dcs.st-and.ac.uk)

Linear aspects of the MHD wave dynamics in the spherically stratified open corona are well understood. The density stratification and magnetic field divergence affect the radial dependence of the Alfvén speed. In particular, this leads to reflection of low frequency Alfvén waves from the inhomogeneity (e.g. An et al. 1990) or, more precisely, from regions where the Alfvén speed increases steeply with distance from the Sun. Alfvén waves of higher frequencies are propagating through the inhomogeneity without significant reflection and can be described by the single wave approximation, or WKB (see, e.g. Hollweg 1990, Barnes 1992, and discussion therein). The stratification affects the propagating waves too, changing the wave amplitude. Moreover, recent consideration of Alfvén wave phase mixing in weakly stratified open magnetic structures has shown that the efficiency of Alfvén wave phase mixing can be dramatically affected by stratification (Ruderman et al. 1998).

The main progress in the understanding of nonlinear spherical Alfvén waves is connected with numerical experiments. Ofman & Davila (1997a) have simulated numerically the evolution of initially monochromatic weakly nonlinear Alfvèn waves in a radially divergent, gravitationally stratified magnetic structure in an isothermal plasma with an enhancement in the Alfvèn speed in the transverse direction. Such a structure can be considered as a vertically stratified magnetic flux tube. It was found that the Alfvèn waves quickly generate longitudinal motions, with sharp asymmetric gradients, which possessed solitary wave properties. The longitudinal waves propagate at supersonic phase speed. Peaks of perturbations of the longitudinal velocity and density were found to be in phase. The distance between the peaks increases with the Alfvèn speed. These soliton-like structures were interpreted by authors as a sequence of slow magnetoacoustic solitons. Parametric studies showed that the solitary waves (which, actually, should be called "cnoidal" waves) occur in a broad range of simulation parameters (Ofman & Davila 1998).

Torkelsson & Boynton (1998) have numerically simulated spherical nonlinear linearly polarized Alfvén waves in a spherically stratified static atmosphere. The attention was concentrated on 1D effects. Wave frequencies exceeded the Alfvén wave cut-off frequency, so the waves were propagating. As in the simulations of Ofman & Davila (1997a, 1998), the Alfvén waves were found to self-interact through nonlinearly generated longitudinal motions and perturbations of the density, steepening into shock waves. Torkelsson & Boynton (1998) argued against the interpretation of these waves as solitons, based on the fact that the same kind of waves showed up in one-dimensional simulations, in which solitary waves could not appear. (However, the solitary waves can be actually auto-waves or dissipative solitons (see, e.g. Nakariakov & Roberts 1999), formed by a balance between geometrical amplification and dissipation.) A significant fraction of the Alfvén wave energy was found to be dissipated. The authors also reported the appearance of oscillations at frequency lower than the driven frequency, which were interpreted as beating between the frequencies of the incident and nonlinearly generated reflected Alfvén waves. In the nonlinear case, in the presence of the induced longitudinal motions, these frequencies do not coincide with each other and the beating appears.

In this paper, we investigate the combined effect of spherical stratification, finite amplitude and dissipation on the propagation of Alfvén waves. These three effects are supposed to be weak, modifying the wave amplitude and shape slowly with height and time. This allows us to apply the method of slowly varying amplitudes and derive an evolutionary equation for the waves. The analytical approach allows us to extract the main features of the dynamics and investigate the physical mechanisms responsible for the wave evolution. In Sect. 2, the model and governing equations considered are discussed. The derivation of an evolutionary equation, which is a spherical analog of the Cohen–Kulsrud–Burgers equation is presented in Sect. 3. Solutions of the equation are discussed in Sect. 4. In Sect. 5, a discussion of results obtained is presented.

2. The model

We consider a spherically stratified atmosphere permeated by a magnetic field, which models an open magnetic structure of a coronal hole. The magnetic field is assumed to be strictly radial and described by the function

$$B_0(r) = \frac{B_0(R_\odot)R_\odot^2}{r^2}. \tag{1}$$

where the coordinate $R_\odot$ is the solar radius. Of course, we consider the domain $r > R_\odot$ only.

Assuming that the coronal hole plasma is in hydrostatic equilibrium, we have for the density

$$\rho_0(r) = \rho_0(R_\odot)\exp\left(-\frac{R_\odot}{H}\frac{r-R_\odot}{r}\right), \tag{2}$$

where H is the scale height. From (1) and (2), the radial profile of the Alfvén speed C_A is given by

$$C_A(r) = \frac{B_0(R_\odot)R_\odot^2}{r^2[4\pi\rho_0(R_\odot)]^{1/2}}\exp\left(\frac{R_\odot}{2H}\frac{r-R_\odot}{r}\right). \tag{3}$$

The atmosphere is assumed to be isothermal, with constant temperature T and sound speed C_s.

Both the scale height H and sound speed C_s are determined by the temperature T. In the solar corona, one can use estimations $H(\mathrm{Mm}) = 50T(\mathrm{MK})$ and $C_s(\mathrm{Mm\,s^{-1}}) = 0.152\,T^{1/2}(\mathrm{MK})$.

There are three independent spatial scales in the problem considered, the radius of the Sun $R_\odot$, the wavelength λ and the density scale height H. The characteristic scale of the Alfvén speed variations r_A which can be defined as $C_A(\mathrm{d}C_A/\mathrm{d}r)^{-1}$, can be expressed through $R_\odot$ and H as

$$r_A \propto \frac{r^2 H}{|4rH - R_\odot^2|}. \tag{4}$$

For typical coronal conditions $T \approx 1.0$–$1.3\,\mathrm{MK}$ and, consequently, $H \ll R_\odot$. Also, in the spatial domain considered, we can take $R_\odot < r < 10R_\odot$. Under these assumptions, we obtain $r_A \approx H$.

As the governing set of equations, magnetohydrodynamics is used,

$$\rho\left[\frac{\partial \mathbf{V}}{\partial t}+(\mathbf{V}\cdot\nabla)\mathbf{V}\right]= -\nabla p-\frac{1}{4\pi}\mathbf{B}\times\mathrm{curl}\,\mathbf{B}-\nabla\times(\rho\nu\nabla\times\mathbf{V}),$$

$$\frac{\partial \mathbf{B}}{\partial t}=\mathrm{curl}\,(\mathbf{V}\times\mathbf{B}),\qquad \mathrm{div}\ \mathbf{B}=0, \tag{5}$$

$$\frac{\partial \rho}{\partial t}+\mathrm{div}(\rho\mathbf{V})=0,$$

where ν is the kinematic viscosity and other notations are standard. Only shear viscosity, which affects Alfvén waves, is taken into account. Although compressive viscosity can affect the Alfvén waves indirectly, affecting compressive waves generated nonlinearly by the Alfvén waves, the effect is weak and is not considered here. We do not have reliable information about the radial dependence of the viscosity coefficient in coronal holes so here the viscosity is assumed to be constant. Also, the induction equation should contain resistivity. However, viscosity and resistivity affect the steepening of the Alfvén waves in a similar way (Ofman et al. 1994). Consequently, finite resistivity does not introduce new physical effects and can be neglected with respect to the viscosity when the Lundquist number is much larger than the Reynolds number. This may occur in the corona if small scale turbulence is present, and the viscosity is enhanced. In these studies we neglect the effects of finite resistivity on Alfvén waves.

Eq. (5) have to be supplemented by the equation of state, $p=C_s^2\rho$. In this model the effects of kinetic pressure anisotropy are neglected since they are believed to be small for the coronal Alfvén waves (e.g. Nakariakov & Oraevsky 1995).

3. The evolutionary equation

Linearly polarized Alfvén waves propagating along the radial magnetic field are described by the equations

$$\rho_0\frac{\partial V_\phi}{\partial t}-\frac{B_0}{4\pi}\frac{1}{r}\frac{\partial}{\partial r}\left(rB_\phi\right)=N_1, \tag{6}$$

and

$$\frac{\partial B_\phi}{\partial t}-\frac{1}{r}\frac{\partial}{\partial r}\left(rB_0V_\phi\right)=N_2, \tag{7}$$

where V_ϕ and B_ϕ are transverse components of the perturbation velocity and magnetic field, respectively, and

$$N_1=-\frac{1}{r^2}\frac{\partial}{\partial r}\left[r^2(\rho_0+\rho)V_\phi V_r\right]-\frac{\partial}{\partial t}(\rho V_\phi) -(\rho_0+\rho)\frac{V_\phi V_r}{r}+\frac{1}{r}\frac{\partial}{\partial r}\left[(\rho_0+\rho)\nu\frac{\partial}{\partial r}(rV_\phi)\right]$$

$$N_2=-\frac{1}{r}\frac{\partial}{\partial r}(rB_\phi V_r).$$

Eqs. (6) and (7) have to be supplemented by equations for perturbations of the density and the longitudinal component of the velocity,

$$\frac{\partial \rho}{\partial t}+\frac{1}{r^2}\frac{\partial}{\partial r}\left(r^2\rho_0V_r\right)=0, \tag{8}$$

$$\rho_0\frac{\partial V_r}{\partial t}+C_s^2\frac{\partial \rho}{\partial r}+g\rho=-\frac{1}{4\pi r}B_\phi\frac{\partial}{\partial r}(rB_\phi)+\rho_0\frac{1}{r}V_\phi^2. \tag{9}$$

Here we assumed that the perturbations of ρ and V_r were initially absent from the system, and were generated nonlinearly by the Alfvén wave. Consequently, only nonlinear terms containing B_ϕ and V_ϕ had to be taken into account. Second order nonlinear terms containing ρ and V_r are neglected, because they are responsible for fourth and higher order nonlinear effects on the Alfvén waves, which are not considered in these studies. Also, we neglect the effects of viscosity on the forced perturbations of density and longitudinal motions.

Eqs. (6) and (7) can be combined into the wave equation

$$\frac{\partial^2 V_\phi}{\partial t^2}-\frac{B_0(r)}{4\pi\rho_0(r)r}\frac{\partial^2}{\partial r^2}\left[rB_0(r)V_\phi\right] =\frac{1}{\rho_0(r)}\left[\frac{\partial N_1}{\partial t}+\frac{B_0}{4\pi r}\frac{\partial}{\partial r}\left(rN_2\right)\right]. \tag{10}$$

The linear terms on the left hand side of this equation coincide with the equation shown in Ofman & Davila (1998) for linear spherical Alfvén waves.

In the following, we restrict our derivation to short wavelength motions, $\lambda\ll H$ and, consequently, $\lambda\ll R_\odot$ and r_A. This restriction allows us to treat the effect of the stratification as a small perturbation. Nonlinear effects are assumed to be weak too, viz. $B_\phi/B_0\ll 1$.

Neglecting terms proportional to $1/R_\odot$ with respect to terms proportional to $1/\lambda$, we rewrite equations (10) as

$$\frac{\partial^2 V_\phi}{\partial t^2}-C_A^2(r)\frac{\partial^2 V_\phi}{\partial r^2} =-\frac{2C_A^2(r)}{r}\frac{\partial V_\phi}{\partial r}+\frac{1}{\rho_0(r)}\left[\frac{\partial \tilde{N_1}}{\partial t}+\frac{B_0}{4\pi}\frac{\partial \tilde{N_2}}{\partial r}\right], \tag{11}$$

with

$$\tilde{N_1}=\frac{B_0}{4\pi r}B_\phi-\frac{\partial}{\partial t}(\rho V_\phi)-\rho_0\frac{\partial}{\partial r}(V_\phi V_r)+\rho_0\nu\frac{\partial^2 V_\phi}{\partial r^2},$$

$$\tilde{N_2}=\frac{1}{r}\frac{\mathrm{d}}{\mathrm{d}r}(rB_0)V_\phi+\frac{\partial}{\partial r}(B_\phi V_r).$$

Note that the expressions $\tilde{N_1}$ and $\tilde{N_2}$ include appropriate nonlinear terms from N_1 and N_2 together with the linear terms which come from the left hand side of Eq. 10.

In addition, from Eqs. (8) and (9) we obtain

$$\rho_0\frac{\partial V_r}{\partial t}+C_s^2\frac{\partial \rho}{\partial r}=-\frac{B_\phi}{4\pi}\frac{\partial B_\phi}{\partial r}, \tag{12}$$

$$\frac{\partial \rho}{\partial t}+\rho_0\frac{\partial V_r}{\partial r}=0, \tag{13}$$

which allow us to determine the value ρ and V_r required for $\tilde{N_{1,2}}$ as functions of V_ϕ (or B_ϕ).

As discussed above, the effects of stratification and nonlinearity are taken to be weak and, consequently, the right hand side of Eq. (11) is smaller than the left hand side. This allows us to apply the method of slowly varying amplitudes. Considering a wave propagating in the positive r-direction, we change the independent variables to

$$\tau = t - \int \frac{\mathrm{d}r}{C_A}, \qquad R = \epsilon r, \tag{14}$$

where ϵ is a small positive parameter of order of the nonlinearity and inhomogeneity,

$$\epsilon \approx \frac{B_\phi}{B_0}, \frac{\lambda}{R_\odot}, \frac{\lambda}{H}.$$

The background variables B_0 and ρ_0 depend on the "slow" coordinate R.

Using these new variables, Eq. (11) is rewritten as

$$2C_A\frac{\partial^2 V_\phi}{\partial\tau\partial R} + C_A\left[C_A\frac{\mathrm{d}}{\mathrm{d}R}\left(\frac{1}{C_A}\right) - \frac{2}{R}\right]\frac{\partial V_\phi}{\partial\tau} = \frac{1}{\rho_0}\frac{\partial}{\partial\tau}\left[\tilde{N_1} - \frac{B_0}{C_A 4\pi}\tilde{N_2}\right], \tag{15}$$

where

$$\tilde{N_1} = -\frac{B_0^2}{C_A 4\pi R}V_\phi + \frac{\rho_0\nu}{C_A^2}\frac{\partial^2 V_\phi}{\partial r^2}, \tag{16}$$

$$\tilde{N_2} = \frac{1}{R}\frac{\mathrm{d}}{\mathrm{d}R}(RB_0)V_\phi - \frac{B_0}{2(C_A^2 - C_s^2)C_A}\frac{\partial V_\phi^3}{\partial\tau}. \tag{17}$$

Perturbations of other physical variables are expressed through ρ as

$$B_\phi = -\frac{B_0}{C_A}V_\phi, \quad V_r = \frac{C_A}{2(C_A^2 - C_s^2)}V_\phi^2,$$

$$\rho = \frac{\rho_0}{2(C_A^2 - C_s^2)}V_\phi^2. \tag{18}$$

Integrating equation (15) with respect to τ and taking the integration constant to be zero, we arrive at the evolutionary equation

$$\frac{\partial V_\phi}{\partial R} - \frac{R_\odot^2}{4H}\frac{1}{R^2}V_\phi - \frac{1}{4C_A(C_A^2 - C_s^2)}\frac{\partial V_\phi^3}{\partial\tau} - \frac{\nu}{2C_A^3}\frac{\partial^2 V_\phi}{\partial\tau^2} = 0. \tag{19}$$

Eq. (19) is an analog of the scalar Cohen–Kulsrud–Burgers equation for the case of spherical geometry.

In the following analysis, it is convenient to use normalized variables,

$$R = R_\odot R', \quad \tau = R_\odot/C_A(R_\odot)\tau', \quad V_\phi = C_A(R_\odot)V_\phi'. \tag{20}$$

Below, the primes are omitted. In the normalized variables, Eq. (19) is written as

$$\frac{\partial V_\phi}{\partial R} - \frac{1}{4HR^2}V_\phi - \frac{1}{4C_A(C_A^2 - C_s^2)}\frac{\partial V_\phi^3}{\partial\tau} - \frac{\bar{\nu}}{2C_A^3}\frac{\partial^2 V_\phi}{\partial\tau^2} = 0, \tag{21}$$

where both the Alfvén and sound speeds are measured in units of the Alfvén speed at the base of the corona, $C_A(R_\odot)$, the scale height H is measured in units of the solar radius, and the normalized viscosity $\bar{\nu} = \nu/[R_\odot C_A(R_\odot)]$ is introduced. The background Alfvén speed is re-written in the dimensionless form as

$$C_A(R) = \frac{1}{R^2}\exp\left(\frac{1}{2H}\frac{R-1}{R}\right). \tag{22}$$

4. Alfvén wave dynamics

Eq. (21) does not have obvious exact solutions. However, qualitative analysis gives us some important insight into the dynamics of spherical weakly nonlinear and weakly dissipative short wavelenghts Alfvén waves.

When the wave amplitude and viscosity are negligible, the last two terms can be dropped and Eq. (21) has the solution

$$V_\phi = V_\phi(1)\exp\left(\frac{R-1}{4HR}\right) \tag{23}$$

showing that the amplitude of an upwardly propagating linear Alfvén wave grows with height. (We must note that expression (23) was derived under the assumption that $\lambda \ll H \ll R_\odot$ and, consequently, consideration of the limiting case of the non-stratified atmosphere, $H \to \infty$, is meaningless.) Thus, the second term in evolutionary Eq. (21) leads to amplification of the Alfvén waves, which can be understood by simple geometrical reasoning (see also, Ofman & Davila 1998, Torkelsson & Boynton 1998). In the absence of dissipation and backward waves, the radial component of the Poynting flux $\mathbf{S} \propto \mathbf{B}\times\mathbf{V}\times\mathbf{B}$ is proportional to $1/r^2$. On the other hand, the radial component is given by the expression $S_r \propto B_0 V_\phi B_\phi$, or, taking into account (1) and (18), $S_r \propto V_\phi^2 B_0^2/C_A$. Consequently, the combination $B_0 V_\phi^2/C_A$ is constant, which gives us

$$V_\phi \propto [C_A(r)/B_0(r)]^{1/2} = \rho_0^{-1/4}(r), \tag{24}$$

which coincides with the expression (23).

The third and fourth terms in the Eq. (21) describe the nonlinear distortion of the wave profile through the generation of higher harmonics and the dissipation. When all three terms are comparable with each other, the dynamics of the Alfvén waves is determined by an interplay between the geometrical amplification, nonlinear generation of higher harmonics and dissipation.

Fig. 1 shows the typical evolution of a wave generated by a harmonic driver on the solar surface, with distance from the Sun. We can distinguish three main stages of the wave dynamics: the geometrical amplification, wave breaking and enhanced dissipation. Initially, the wave is amplified by the stratification, keeping

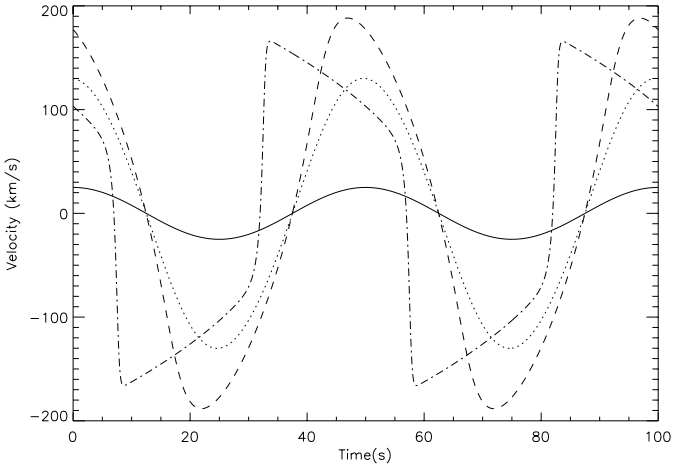

Fig. 1. Evolution of the temporal dependences of the initially harmonic nonlinear spherical Alfvén waves with the distance from the Sun. The solid line shows the variation of the velocity at the solar surface, the dotted line at about 2 $R_\odot$, the dashed line at 5 $R_\odot$, and the dotted-dashed line at 9 $R_\odot$. The initial wave period is 50 s and the amplitude is 25 km s^{-1}. The atmosphere is isothermal with $T = 1.4$ MK and the Alfvén speed near the base of the corona is 1000 km s^{-1}.

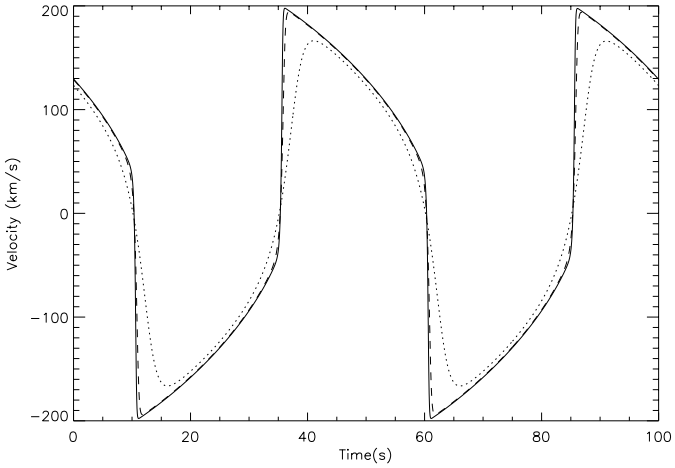

Fig. 2. The shape of an Alfvén wave at 8 solar radii for three different dimensionless viscosities $\bar{\nu} = 5. \times 10^{-6}$ (the solid line), $\bar{\nu} = 1. \times 10^{-5}$ (the dotted line) and $\bar{\nu} = 5. \times 10^{-5}$ (the dashed line). The initial wave period is 50 s and the amplitude is 25 km s^{-1}. The Alfvén speed is taken to be 1000 km s^{-1} near the base of the corona.

nearly the same harmonic shape. When the amplitude reaches a certain value, nonlinear effects become more pronounced and the wave steepens. The shape of the wave evolves to the typical shape described by the scalar Cohen–Kulsrud equation. When the wave steepens, dissipation comes into play and the wave shows intensive decay. Also, in this stage, the nonlinear wave accelerates, propagating faster than the local Alfvén speed. (The wave maxima and nodes shift to the left).

This scenario of the wave evolution is almost independent of the specific value of the viscosity $\bar{\nu}$, provided the viscosity is sufficiently weak ($\bar{\nu} < 10^{-5}$ for the parameters considered). Fig. 2 shows the wave shape in the nonlinear dissipation stage for three different values of the viscosity, 10^{-5}, 5×10^{-5} and 5×10^{-6}. The wave shape remains almost the same for all three values of the viscosity, with only a slight decrease for the case of stronger dissipation. Also, for stronger dissipation the wave is smoother in the vicinity of wave fronts. This independence of the wave evolution on the viscosity allows us to conclude that the wave shows a similar behavior in cases of smaller viscosities, which are difficult to model numerically.

Figs. 3–5 show the dependence of the wave amplitude on the height for different parameters of the waves and the corona: wave amplitudes (Fig. 3), wave periods (Fig. 4) and atmosphere temperatures (Fig. 5). It is seen in Fig. 3, that, for higher amplitudes, the stage of nonlinear dissipation begins earlier and the following dissipative decrease of the amplitude is steeper than for lower initial wave amplitudes. The transverse velocity reaches its maximum value up to 200 km s^{-1} at 7–9 solar radii, for various initial amplitudes (15–25 km s^{-1} for runs performed). The maximum amplitude is also connected with the wave frequency, as seen in Fig. 4. Higher frequency waves reach their amplitude maxima at shorter distances. However, lower frequency waves reach higher overall maximum amplitudes.

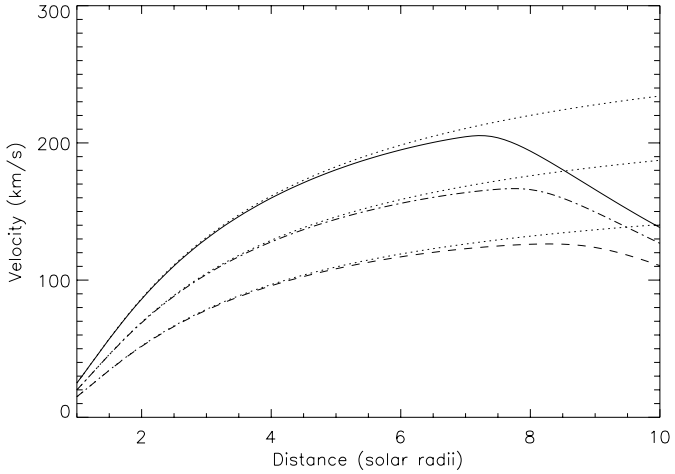

Fig. 3. Dependence of the nonlinear spherical Alfvén wave amplitude on the distance from the Sun for three different initial amplitudes A. The solid line corresponds to $A = 25$ km s^{-1}, the dash-dotted line to $A = 20$ km s^{-1} and the dashed line to $A = 15$ km s^{-1}. The dotted curves show the growth of the waves according to linear solution (23). The initial wave period is 50 s. The atmosphere is isothermal with $T = 1.4$ MK and the Alfvén speed near the surface is 1000 km s^{-1}.

Fig. 5 shows that the maximum amplitude is quite sensitive to the temperature of the atmosphere. From Eq. (19), it follows that the coefficient of the nonlinear term, which determines the nonlinear steepening, depends on the temperature in two different ways: directly, through the sound speed C_s, and indirectly through the scale height H, which determines the radial dependence of the density ρ_0 and, consequently, the Alfvén speed C_A. In the cooler atmosphere, the Alfvén waves reach higher amplitudes. The position of the wave breaking and the nonlinear dissipation do not depend strongly on the temperature.

Figs. 6 and 7 show driven perturbations of density and longitudinal velocity, respectively, for three different temperatures

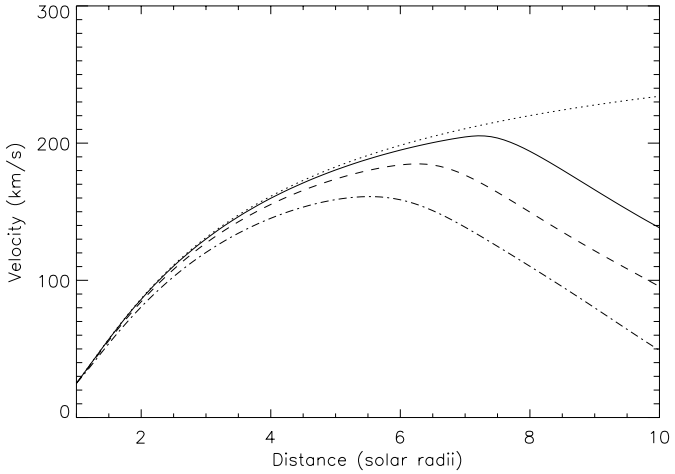

Fig. 4. Dependence of the nonlinear spherical Alfvén wave amplitude on the distance from the Sun for three different wave periods P. The solid line corresponds to $P = 50$ s, the dashed line to $P = 25$ s and the dotted-dashed line to $P = 15$ s. The dotted curve correspond to linear solution (23). The initial wave amplitude is 25 km s^{-1}. The atmosphere is isothermal with $T = 1.4$ MK and the Alfvén speed near the base of the corona is 1000 km s^{-1}.

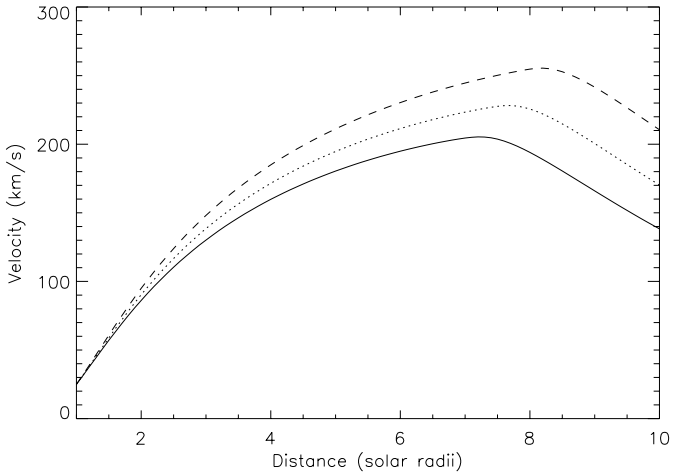

Fig. 5. Dependence of the nonlinear spherical Alfvén wave amplitude on the distance from the Sun for three different temperatures T of the isothermal atmosphere. The solid line corresponds to $T = 1.4$ MK, the dotted line to $T = 1.35$ MK and the dashed line to $T = 1.3$ MK. The initial wave period is 50 s and the amplitude is 25 km s^{-1}. The Alfvén speed is 1000 km s^{-1} near the base of the corona.

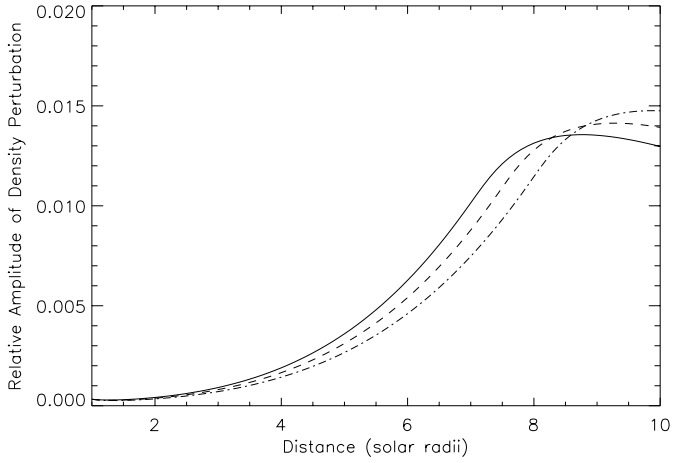

Fig. 6. Dependence of relative perturbation of density generated by nonlinear Alfvén waves, on the distance from the Sun, for three different temperatures T of the isothermal atmosphere. The solid line corresponds to $T = 1.4$ MK, the dashed line to $T = 1.35$ MK and the dash-dotted line to $T = 1.3$ MK. The initial wave period is 50 s and the amplitude is 25 km s^{-1}. The Alfvén speed is taken 1000 km s^{-1} near the base of the corona.

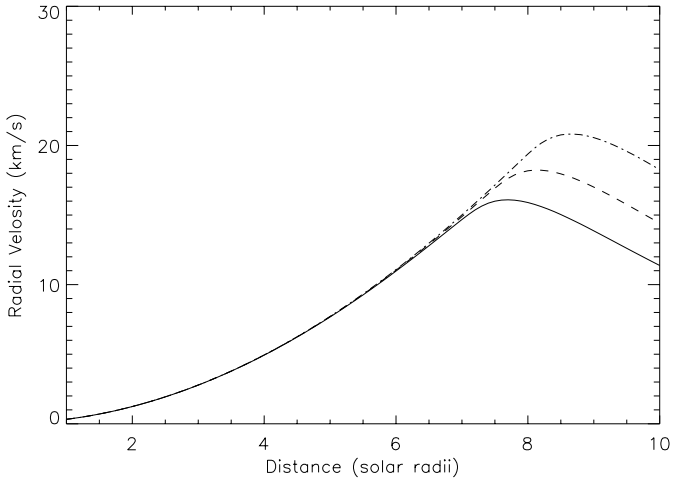

Fig. 7. Longitudinal motions generated by nonlinear Alfvén waves as a function of the distance from the Sun, for three different temperature T of the isothermal atmosphere. The solid line corresponds to $T = 1.4$ MK, the dashed line to $T = 1.35$ MK and the dash-dotted line to $T = 1.3$ MK. The initial wave period is 50 s and the amplitude is 25 km s^{-1}. The Alfvén speed is 1000 km s^{-1} near the base of the corona.

of the atmosphere. The driven perturbations are connected with the amplitude of Alfvén waves by expressions (18). The evolution of the driven perturbations follows the growth of the Alfvén wave amplitude. For typical parameters, $C_A = 1000$ km s^{-1}, $P = 50$ s, $T = 1.4$ MK and $A = 25$ km s^{-1}, the driven density perturbations reach 1.5% of the background density, while the longitudinal speed reaches 15–20 km s^{-1}. The amplitudes of the driven perturbations of the density and the longitudinal velocity are sensitive to the temperature of the atmosphere and are strongest for lower temperatures. It can be explained qualitatively: lower temperatures correspond to smaller density scale heights, which leads to stronger geometrical amplification according to Eq. (23); a higher amplitude wave is more nonlinear and drives the density and the longitudinal velocity perturbations more efficiently.

5. Discussion

We have shown that dynamics of nonlinear spherical linearly polarized, small amplitude Alfvén waves in a stratified and dissipative plasma of coronal holes is described by spherical scalar Cohen–Kulsrud–Burgers Eq. (19). Analysis of the equation al-

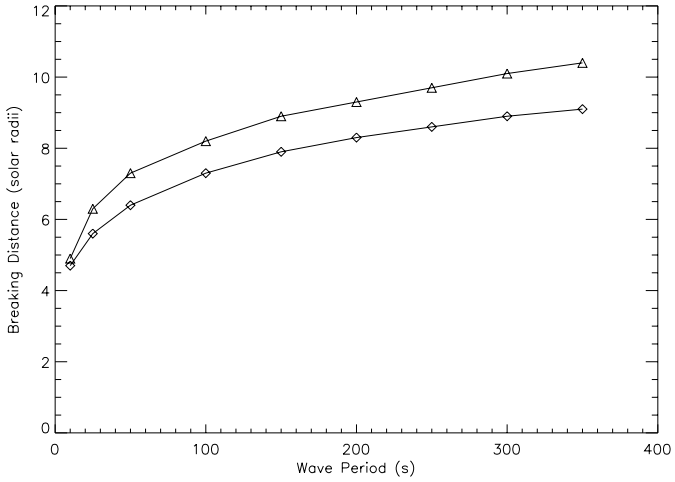

Fig. 8. Dependence of the breaking distance of Alfvén waves on the wave period. The curve with triangles corresponds to the amplitude 25 km s^{-1} near the surface and with diamonds to 35 km s^{-1}. The temperature is 1.4 MK and the Alfvén speed is 1000 km s^{-1} near the base of the corona.

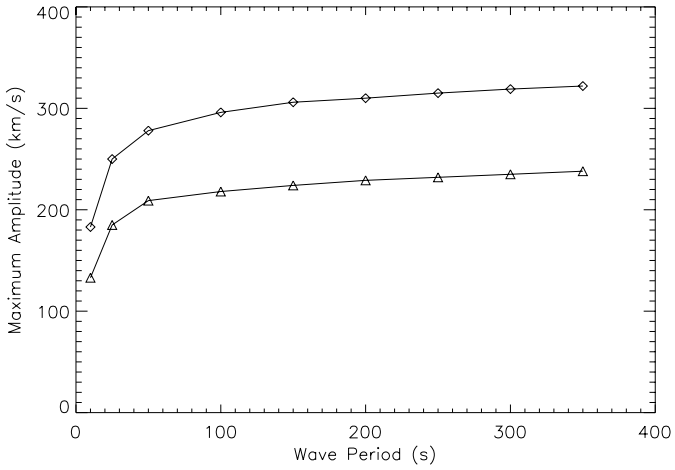

Fig. 9. Dependence of the maximum amplitude of an Alfvén wave upon the wave period for parameters of Fig. 8.

lows us to investigate an interplay of the effects of nonlinearity, stratification and dissipation on the wave dynamics. We found that linearly polarized Alfvén waves of weak amplitude (2–3% of the background Alfvén speed at the base of the corona) and long periods (up to 300 s) are subject to nonlinear steepening and efficient nonlinear dissipation, which is almost independent of the value of the shear viscosity (when $\bar{\nu} < 10^{-5}$), in the low corona (less than 10 $R_\odot$). These results confirm previous numerical findings (e.g. Ofman & Davila 1997a, 1998; Torkelsson & Boynton 1998) and provide us with a powerful tool for parametric studies of the Alfvén wave dynamics, allowing us to extract the main physical mechanisms responsible for the dynamics.

Domains of applicability of the theory developed can be estimated as follows. The wavelength λ of the waves considered is smaller than the density scale height H, $\lambda \ll H$. Consequently, the theory works for waves with periods less then H/C_A. For $T = 1.3$ MK and $C_A = 1000$ km s^{-1}, the period has to be much less than 65 s. (Practically, according to Tu & Marsch (1995), the criteria can be much weaker, $\lambda \ll 4\pi H$, and, consequently, waves of much longer periods can be described too). Also, full MHD numerical simulations did not show any significant reflection for wave periods shorter than 300 s, so the application of the WKB approximation for waves with these periods is justified.

Eq. (19) obviously does not work when the Alfvén speed C_A is approaching the sound speed C_s. The single wave approximation brakes down at this distance and interaction between Alfvén and sound waves has to be considered in this case. Consequently, equation (19) is applicable in the low-β parts of coronal holes only, at distances less than 15–20 solar radii.

The value of the viscosity remains an unknown parameter. According to Braginskii's theory, for the typical coronal hole conditions: the concentration 10^8 cm^{-3}, the temperature $T = 1.4$ MK and the magnetic field 5 G, the dynamic shear viscosity is $\eta \approx 1.9 \times 10^{-13}$ g (cm s)$^{-1}$, which gives us the kinematic viscosity $\nu = \eta/\rho_0 \approx 1.14 \times 10^3$ cm^2 s^{-1} and $\bar{\nu} \approx 1.6 \times 10^{-16}$. According to our results, this number would lead to extremely sharp gradients in the wave fronts. Nevertheless, the wave evolution and nonlinear dissipation turn out to be nearly independent of the dissipation (see Fig. 2) and the results obtained above with much higher dissipation ($\bar{\nu} \approx 10^{-5}$) may still be valid. We note that, the viscosity and the resistivity can be drastically enhanced by plasma turbulence (Nakariakov et al. 1999).

In this study, we neglected an alternative nonlinear damping process which affects Alfvén waves. This is the decay of the Alfvén waves into another Alfvén wave, traveling in the opposite direction, and a slow magnetoacoustic wave. Slow waves are subject to much stronger dissipation and, consequently, can be an indirect sink for Alfvén wave energy. However, according to Cohen & Dewar (1974), efficiency of such a process is low. Consequently, the process can be neglected.

The results obtained above show that nonlinear dissipation of the Alfvén waves can significantly contribute to heating of the coronal hole plasma and solar wind acceleration at distances less than 10 solar radii. The thermodynamic aspects of these studies will be discussed elsewhere in more detail. Here, we discuss implications of the theory developed for coronal seismology. Propagation of the Alfvén waves outward from the Sun is accompanied by two effects which can be observed: (a) the increase of the wave amplitude, contributing to non-thermal broadening of emission lines by the line-of-sight Doppler broadening, with distance from the Sun, and (b) appearance of the breaking point, corresponding to the maximum wave amplitude (after this point the wave is subject to very efficient nonlinear dissipation). Figs. 8 and 9 show the dependence of the breaking point position upon the wave period. It is seen that for waves with periods less than 400 s and amplitudes at the base of the corona over 25 km s^{-1}, the breaking point is closer than 10 solar radii to the Sun. Determination of the position of the breaking point by measurement of distance of the strongest non-thermal broadening would provide us with a unique tool for the determination of the unresolved spectrum of the Alfvén waves. Such

an information would be of crucial importance for the coronal physics.

According to Fig. 8, if all the other parameters of coronal holes are fixed, the breaking distance is determined by the amplitude and the period of the wave. Waves of shorter periods break closer to the base of the corona. Alfvén waves with short (less than 10 s) periods break strongly and are dissipated within 1–3 solar radii.

In addition, we would like to note that our results are applicable not only for the physics of coronal holes, but also for other astrophysical situations, such as the problem of the support of molecular clouds by Alfvén waves. This subject will be discussed elsewhere.

Acknowledgements. One of the authors (VMN) is grateful to B. Roberts and M.S. Ruderman for a number of stimulating discussions. LO would like to thank the NASA SR&T program (NASW-98004), the NASA SOHO Guest Investigator program (NASW-98024), the NASA Space Physics Theory program, and the ISTP program. The authors are grateful to the referee, U. Torkelsson for valuable comments.

References

An C.-H., Suess S.T., Moore R.L., Musielak Z.E., 1990, ApJ 350, 309
Balogh A., Smith E.J., Tsuritani B.T., et al., 1995, Science 268, 1007
Barnes A., 1992, J. Geophys. Res. 97, 12105
Cohen R.H., Dewar R.L., 1974, J. Geophys. Res. 79, 4174
Cohen R.H., Kulsrud R.M., 1974, Phys. Fluids **17**, 2215
Deforest C.E., Gurman J.B., 1998, ApJ 501, L217
Heyvaerts J., Priest E.R., 1983, A&A 117, 220
Hollweg J.V., 1971, J. Geophys. Res. 76, 7491
Hollweg J.V., 1990, J. Geophys. Res. 95, 14873
Kennel C.F., Blandford R.D., Wu C.C., 1990, Phys. Fluids B 2, 253
Nakariakov V.M., Ofman L., DeLuca E.E., Roberts B., Davila J.M. 1999 Science 285, 862
Nakariakov V.M., Oraevsky V.N., 1995, Solar Phys. 158, 29
Nakariakov V.M., Roberts B., 1999, Phys. Letters A 254, 314
Nakariakov V.M., Roberts B., Murawski K., 1997, Solar Phys., 175, 93
Nakariakov V.M., Roberts B., Murawski K., 1998, A&A 332, 795
Ofman L., Davila J.M., 1997a, ApJ 476, 3570
Ofman L., Davila J.M., 1997b, ApJ 476, L51
Ofman L., Davila J.M., 1998, J. Geophys. Res. 103, 23677
Ofman L., Davila J.M., Steinolfson R.S., 1994, ApJ 421, 360
Ofman L., Nakariakov V.M., Deforest C.E., 1999, ApJ 514, 441
Ofman L., Romoli M., Poletto G., Noci G., Kohl J.L., 1998, ApJ 507, L189
Parker E.N., 1965, Space Sci. Rev. 4, 666
Ruderman M.S., Nakariakov V.M., Roberts B., 1998, A&A 338, 1118
Torkelsson U., Boynton G.C., 1998, Mon. Not. R. Astron. Soc. 295, 55
Tu C.-Y., Marsch E., 1995, Space Science Reviews, 73, 1